TDR 2006

Purdue University

Soil Texture Characterization from TDR Waveform Analysis

Carlos E. Zambrano, Vincent P. Drnevich, Xiong Yu, and Robert Nowack

Ref.: Zambrano, Carlos E., Drnevich, Vincent, P., Yu, Xiong, Nowack, Robert, "Soil Texture Characterization from TDR Waveform Analysis", Proc. TDR 2006, Purdue University, West Lafayette, USA, Sept. 2006, Paper ID 1, 21 p., https://engineering.purdue.edu/TDR/Papers

Soil Texture Characterization from TDR Waveform Analysis

Carlos E. Zambrano[1], Vincent P. Drnevich[2], Xiong Yu[3], and Robert Nowack[4]

[1] Geotechnical Engineer, MWH Global, 175 W. Jackson Blvd., Suite 1900, Chicago, IL 60604-2814; PH (312) 831-3815; email: carlos.e.zambrano@mwhglobal.com.

[2] Professor of Civil Engineering, Purdue University, School of Civil Engineering, 550 Stadium Mall Dr., West Lafayette, IN 47907-2051; PH (765) 494-5029; FAX (765) 494-5029; email: drnevich@purdue.edu.

[3] Assistant Professor, Department of Civil Engineering, Case Western Reserve University, 10900 Euclid Avenue, Bingham 210, Cleveland, OH 44106-7201; PH (216) 368-6247; FAX (216) 368-5229 email: xxy21@po.cwru.edu.

[4] Professor, School of Earth and Atmospheric Sciences, Purdue University, 550 Stadium Mall Dr., West Lafayette, IN 47907-2051; PH (765) 494-5978; FAX (765) 496-1210 email: nowack@purdue.edu.

Abstract

The dispersive electromagnetic (EM) behavior of soils is strongly related to the mineralogy, soil structure, and pore fluid characteristics. However, time domain reflectometry (TDR) measurements (TDR waveforms), for compaction quality control of soils in civil engineering, are predominantly used for soil water content and dry density estimation. These two parameters are calculated based on empirical equations that relate them to the soil dielectric permittivity (K_a) and the bulk electric conductivity (EC_b) (Siddiqui et al., 2000[1]; Yu and Drnevich, 2004[2] and Drnevich et al. 2006[3]). K_a and EC_b are obtained in the time domain from four data points of the TDR waveform, disregarding most of the acquired data (usually 2048 data points) that reflects the EM response of the material over a broad frequency range. The complexity of the soil-water interaction in the presence of a time-varying EM field, and the presence of a non-transverse propagation mode in the TDR system (Zambrano, 2006[4]) limit the characterization of soils by dielectric spectroscopy. This paper presents a semi-empirical method for soil texture identification based on an integrated numerical and experimental analysis of the effect of the EM soil dispersive behavior on TDR waveforms. Evaluation of TDR tests conducted at 20°C on sands, silts, and clays using tap water at different water contents and dry densities shows that a simple time-domain signal processing of the first reflection from the probe section captures the effects of the EM soil-water interaction. Considering that the coefficients of the TDR empirical equations for soil water content and dry density estimation are soil-type dependent, the developed method allows self-calibrating the TDR system. The result of this work provides the basis for using the TDR technique as a potential tool for soil characterization in addition to water content and dry density estimation.

Key Words Time domain reflectometry (TDR), soil texture, soil characterization, dielectric permittivity (K_a), electric conductivity (EC_b), water content, dry density

Introduction

Time domain reflectometry (TDR) recently developed technology in civil engineering for measurements of soil water content and dry density by empirical equations that relate these two parameters with K_a and EC_b. The basic electrical parameters of the soil, K_a and EC_b, are obtained from the travel time of EM wave through the soil and the amplitude of the EM wave after all of the reflections in the TDR system have taken place, respectively (Siddiqui et al., 2000[1]; Yu and Drnevich, 2004[2]; Drnevich et al. 2006[3]; ASTM D6780-05[5]). Evaluation of TDR test on different soil types has showed that the coefficients of the TDR empirical equations are soil-type dependent (Zambrano, 2006[4]). The determination of the soil type by the interpretation of the TDR waveform would then allow self-calibrating the equipment in-situ, and at the same time would make the TDR technique a tool for soil characterization as well.

Although the EM behavior of soils is strongly related to the mineralogy, soil structure, and pore fluid characteristics, the current time-domain interpretation of TDR waveforms is usually limited only to the determination of soil water content and dry density because only local points of the TDR signal are evaluated, disregarding most of the acquired data that reflects the dispersive EM response of the material over a broad frequency range. A comprehensive approach for the extraction of detailed information of the soil being tested is given by dielectric spectroscopy that requires a wave propagation model for a non-uniform transmission line (TL) and a dispersive dielectric model of the insulating material (soil) being tested. However, this approach is limited by the lack of a dielectric model capable of describing the complex EM behavior of wet fine soils at frequencies below 1 GHz (Lin, 2003[6]; Yu et al., 2005[7]), and by the non-transverse propagation mode observed in the TDR TL (Zambrano, 2006[4]). Considering the limitations of the theoretical approach, this paper introduces a semi-empirical method for the identification of soil type based on an integrated numerical and experimental analysis of TDR waveforms for coarse and fine soils with different water contents and dry densities. The experimental work was conducted at 20°C and the soil specimens were prepared with tap water. The result of this work provides the basis for making the TDR technique a tool not only for water content and dry density estimation, but also for soil characterization.

Background

Polarization of Soils

Soil is a multiphase medium consisting of materials that exhibit electronic, ionic and orientational polarization (Santamarina, J.C. 2001[8]). The liquid phase typically exhibits all three forms of polarization. On the other hand, the solid (soil particles) and gas (e.g. air) phases experience only electronic and ionic polarization. Figure 1 shows the schematic representation of the alignment of microscopic dipoles of the soil phases when an external electric field is applied. The dispersive EM behavior of materials is quantitatively described by the equivalent relative permittivity (ε_r*), which is a complex dimensionless parameter given by the ratio of the frequency-dependent dielectric permittivity of the medium (ε*) to the permittivity of the free space ($\varepsilon_o = 8.854 \times 10^{-12}$ farads/meter). The real part of ε* is a measure of how much energy from an external field is stored in a material. The apparent dielectric constant (K_a) from time domain interpretation of TDR waveforms estimates this value at a frequency of approximately 1 GHz

(Heimovaara, 1994[9]). The imaginary part of ε* represents the dielectric loss by radiation, interaction among charges, thermal effects, and electrical conductivity. When a time-varying EM field is applied, like the one generated by TDR devices, there is a phase lag between the polarization vector and the applied field because charges and molecules possess inertia, which makes polarization a dynamic phenomenon with an amplitude and phase that vary with frequency. As the frequency of the applied field increases the alignment of the charges with the field become attenuated. This phenomenon is called dielectric relaxation and is represented by a fast decrease of the real part of ε_r*. The dielectric relaxation of free water occurs at about 17 GHz.

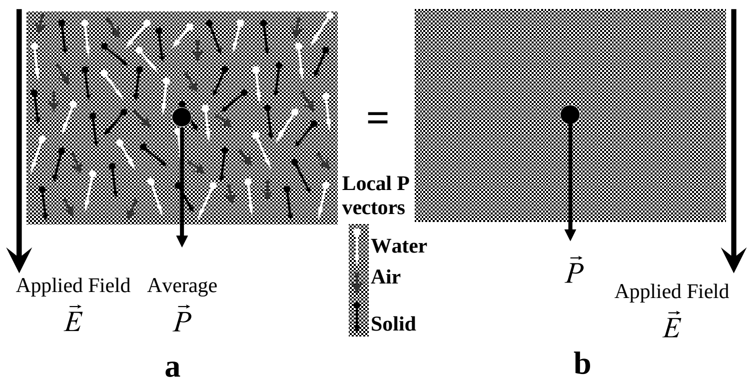

Fig. 1. Schematic representation of soil polarization. a) Microscopic polarization of the individual components. b) Macroscopic polarization. The macroscopic polarization is given by the vectorial sum of all of the microscopic polarization vectors (After Hilhorst et al., 2000[10]).

The simplified schematic of soil polarization presented in Figure 1 does not consider the interfacial effect given by the soil-water interaction, which becomes important as the size of the soil particles decreases and the surface forces become relatively important compared with the mass of the particles. Figure 2 shows a schematic representation of the dispersive EM response of wet soils, which is represented by multiple polarization mechanisms. These include the Maxwell-Wagner relaxation (which occurs in kilohertz range), bound water relaxation (which occurs at megahertz range) and free water relaxation (which occurs in low gigahertz range). Wet clay exhibits all these types of relaxations; wet silt-clay exhibits both bound water relaxation and

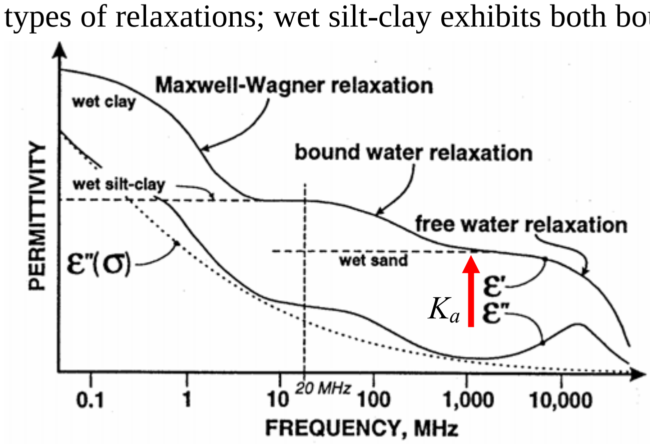

Fig. 2. Schematic dielectric permittivity spectrum of wet soils (Hilhorst and Dirksen, 1994[11]).

free water relaxation; wet sand exhibits only free water relaxation. These are attributed to the types and extent of interactions inside and between the soil particles and water (Figure 2).

EM wave propagation through a TDR system

The Purdue TDR system is a multi-section TL with different insulating materials. The main segments of the TL are represented by four homogenous sections; a front panel (pulse generator/sampler), a 1.8m-long coaxial cable, a multiple rod probe (MRP) head and a probe section, which is designed to have soil as a dielectric material (Figure 3). The front panel generates and sends a step voltage through the TDR system, and records the reflected signal associated with the dielectric properties of the soil being tested and the TL characteristics.

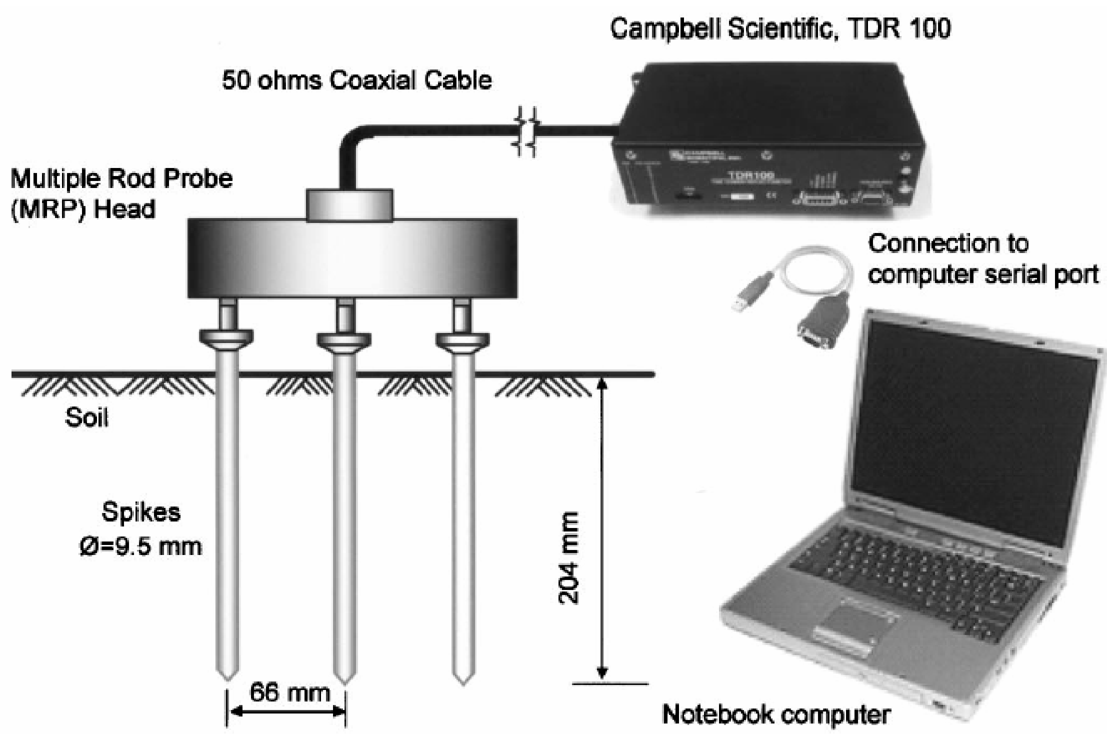

Fig. 3. TDR system components (Yu and Drnevich, 2004[2]).

Figure 4 shows a TDR waveform of a clayey soil. The input step is shown at about 0.5m and has a height of $V_s/2$, where V_s is the source voltage. The fast rise time (< 200 picoseconds) induces high frequency components to the signal. The subsequent flat portion of the signal is associated with the wave traveling forward through the coaxial cable. The first peak marked by *A* is associated with a positive reflection caused by the impedance mismatch between the coaxial cable and the MRP head. The entry of the wavefront through the soil specimen is represented by the negative reflection that follows. When the wavefront reaches the end of the probe (Point *B*), a positive reflection occurs. The TDR waveform beyond this point represents the subsequent travels of the wave through the probe section, which is also composed of high order reflections associated with the multiple reflections in the TL. Point *C* indicates the long-term response of the TDR TL, after all of the multiple reflections in the system have taken place.

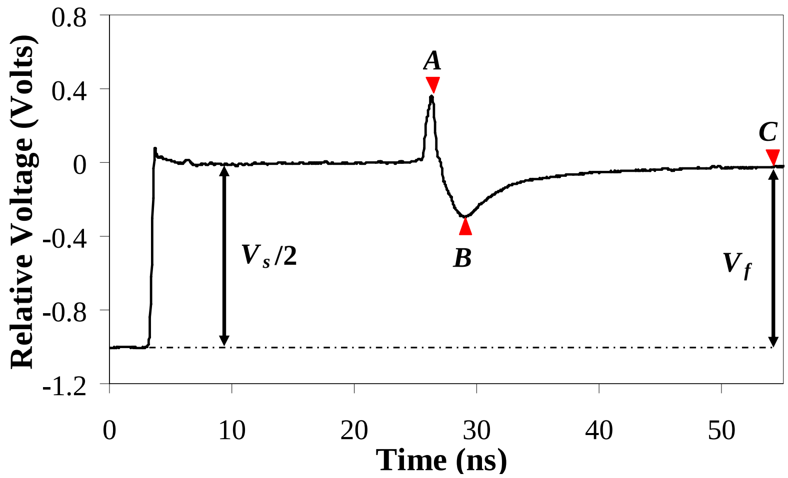

Fig. 4. TDR waveform of a clay soil.

Electromagnetic wave propagation in transmission lines is defined in the frequency domain by the EM Maxwell's equations that describe the interdependence of the electric and magnetic fields. These fields define the voltage between the conductors (V) and the line current (I). As a simplification of the propagation phenomenon, a transverse electromagnetic propagation mode (TEM) is assumed in the analysis of TDR systems. The V and I are then uniquely defined given an EM wavefront perpendicular to the conductors. Feng et al. (1999)[12] and Lin (1999)[13] developed a frequency domain propagation model that accounts for the multiple reflections in the TDR system and the dispersive EM behavior of soils. The model allows determining the sampled voltage by discretizing the TDR TL in a cascade of four uniform segments (e.g. the front panel, coaxial cable, MRP head, and probe section). Considering that the sampled voltage by the TDR oscilloscope is the result of the linear superposition of the launched step voltage and the voltage reflected back, the solution of the sampling voltage can be rewritten in terms of an incident wave and a reflected wave as

$$V(0) = V_{in} + S_{11} V_{in} \tag{1}$$

where S_{11} is the scatter function defined by

$$S_{11} = \frac{Z_{in}(0) - Z_S}{Z_{in}(0) + Z_S} \tag{2}$$

where Z_{in} is the TL equivalent impedance and Z_s is the source impedance of the front panel, which is about 50 Ω.

The term Z_{in} is obtained from the input impedance method that defines an equivalent impedance of the non-homogenous TL using a bottom-up fashion, starting with the boundary condition at the end of the TL (open circuit) and transferring the impedance back successively to the next discontinuity until the input impedance at the sampling point is reached with continuity constraints at the interfaces of the four uniform segments. Equation 3 summarizes the input impedance calculation process.

$$
\begin{aligned}
&Z_{in} = Z_L \\
&Z_{in}\left(z_{n-1}\right) = Z_{c,n}\frac{Z_L + Z_{c,n}\tanh\left(\gamma_n l_n\right)}{Z_{c,n} + Z_L\tanh\left(\gamma_n l_n\right)} \\
&Z_{in}\left(z_{n-2}\right) = Z_{c,n-1}\frac{Z_{in}\left(z_{n-1}\right) + Z_{c,n-1}\tanh\left(\gamma_{n-1} l_{n-1}\right)}{Z_{c,n-1} + Z_{in}\left(z_{n-1}\right)\tanh\left(\gamma_{n-1} l_{n-1}\right)} \\
&\vdots \\
&Z_{in}\left(0\right) = Z_{c,1}\frac{Z_{in}\left(z_1\right) + Z_{c,1}\tanh\left(\gamma_1 l_1\right)}{Z_{c,1} + Z_{in}\left(z_1\right)\tanh\left(\gamma_1 l_1\right)}
\end{aligned}
\tag{3}
$$

where $Z_{c,i}$, γ_i, and l_i are the characteristic impedance, propagation constant, and the length of each uniform section, respectively. Z_{in} (z_{n-1}) is the overall input impedance from the segment n to the end of the TL. In our particular case n is equal to 4. The frequency-dependent terms γ and Z_c are given by

$$\gamma = \frac{\left(j2\pi f\right)}{c}\sqrt{\varepsilon_r *} \tag{4}$$

$$Z_c = \frac{Z_p}{\sqrt{\varepsilon_r *}} \tag{5}$$

where j is $\sqrt{-1}$, f is the frequency, c is the velocity of the EM wave in the free space (2.998x10^8 m/s), and ε_r* and Z_p are the equivalent permittivity of the dielectric and the reference impedance of the TL section under study, respectively. Z_p is defined by the impedance of the TL filled with air. Z_p is then a function of the cross-section of the TL and can be defined, analytically, from EM theory or by calibrating the TL using a material of known dielectric properties as an insulating material of the probe section.

TDR System Calibration

The TL characterization is an inverse problem that consists in the determination of the TL system parameters of an equivalent system that match the EM response of the real system. Z_p, l and ε* constitute the TL system parameters for each TL homogeneous section. For the inversion analysis of the system parameters, the TDR TL was divided into 4 sections; the front panel, coaxial cable, MRP head, and the probe section. The front panel, coaxial cable and MRP head were further subdivided into thirty, three, and two parts, respectively. Two of the TL system parameters were calibrated successively from the front panel to the probe section to reduce the number of unknowns in the calibration inverse analysis. Table 1 presents the TL parameters to be calibrated for each TDR section. The waveforms of the front panel and coaxial cable to be matched were obtained by attaching a 50 Ω impedance block at the end of the cable tester and coaxial cable, respectively. The waveforms of the MRP head of sections 3 and 4 (Table 1) to be matched were obtained by shorting the circuit at the end of these sections. For the calibration of the probe section, this segment was filled with deionized water, which has well documented electric properties (Table 2), in order to concentrate the inversion process on the parameters of the conductor of this segment.

Table 1. Initial condition of the calibration inversion problem. The front panel was modeled by 30 sections. The coaxial cable was modeled by 3 sections.

Section		Unknown	Known
1	Front panel	L_i, Z_{pi}	ε^*_i
2	Coaxial Cable	Z_{pi}, ε^*_i	L_i
3	MRP head section with Delrin® as dielectric material	Z_p, ε^*_i	L
4	MRP head section with Air as dielectric material	Z_p, L	ε^*_i
5	Probe with Deionized water as dielectric material.	Z_p, L *or* Z_p, ε^*	ε^* *or* L

Table 2. Dielectric properties of water (from Heimovaara, 1994[9])

Liquid	T (°C)	ε_s	ε_∞	f_{rel} (GHz)	σ_{dc} S/m
Deionized water	20.6	79.9	4.22	17	0

Note: ε_∞ and ε_s are the dielectric constant at high frequency and at zero frequency, respectively. f_{rel} is the relaxation frequency, and σ_{dc} is the electrical conductivity.

The optimal TL parameters were obtained by minimizing the residual sum-of-square differences between the measured and the simulated waveforms (Feng et al. 1999[12]; Lin, 1999[13] and Lin, 2003[6]). Lin (1999)[13] developed computer codes that perform the calibration inversion analysis using Bayesian statistical methods provided by the Optimization Toolbox of Matlab™. A similar approach was also implemented by Huisman et al. (2002)[14]. Yu et al. (2005)[7] refined the codes developed by Lin (1999)[13] to facilitate data input and enhance the capability of performing analyses regardless of the measurement system. The existing subroutines were extended to perform inversion of all of the calibrated TL system parameters (Table 1) at the same time to refine the estimated calibration model parameters. This last process showed improvements to the fitting of the observed data (e.g. waveform).

Figure 5 shows the estimated impedance profile of the front panel given by the inversion analysis, and Tables 3 and 4 present the TL parameters of the coaxial cable, coaxial head, and probe section. Figure 6 presents the performance of the calibrated parameters for prediction of the deionized water TDR waveform.

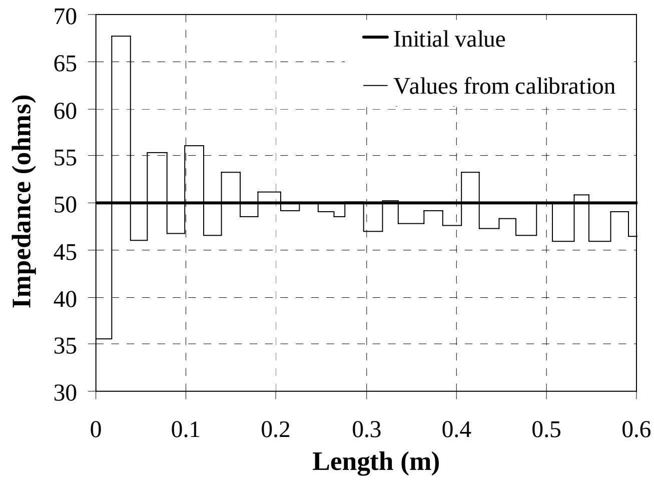

Fig. 5. Impedance profile of the front panel from inversion

Table 3. Transmission line parameters of the coaxial cable. It was subdivided into three segments. Z_p is the reference impedance, l_i is the length of segment i, ε_∞ and ε_s are the dielectric constant at high frequency and low frequency, respectively, f_{rel} is the relaxation frequency, and σ_{dc} is the electrical conductivity at zero frequency

Z_p (Ω)	l_i (m)	ε_s	ε_∞	f_{rel} (Hz)	σ_{dc} (S/m)
71.59	0.3396	2.25	2.26	101.32×10^6	2.07E-10
71.78	0.7997	2.23	2.17	101.38×10^6	8.45E-10
74.37	0.6998	2.32	2.21	101.19×10^6	7.17E-10

Table 4. TL parameters of the MRP head and the probe section. ε_∞ and ε_s are the dielectric constants at high frequency and at low frequency, respectively, f_{rel} is the relaxation frequency, and σ_{dc} is the electric conductivity.

Section	**Z_p (Ω)**	**l_i (m)**	**ε_s**	**ε_∞**	**f_{rel} (Hz)**
CH Delrin® section	198.86	0.0374	3.83	3.76	1.0×10^7
Air gap sections					
Section		Z_p (Ω)	l_i (m)		ε
CH air gap section		104.6	0.057		1
Probe		148.5	0.119		1

Based on experimental observations Zambrano, 2006[4] concluded that a non-TEM occurs at the soil surface level (Figure 3) due to high dielectric contrast between the air and the soil being tested (Paul, 1994[15]). This limitation affects the calibration of the probe section considering the top-to-bottom fashion of the calibration inversion process.

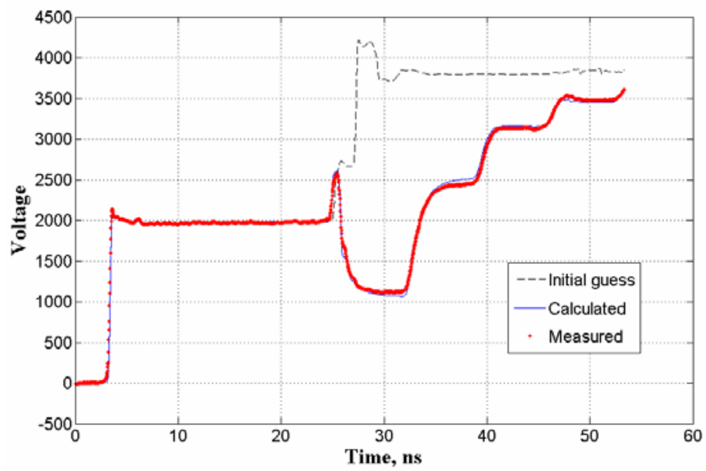

Fig. 6. Measured signal in deionized water versus that from inversion analysis. The voltage axis is scaled by a factor of 2000.

Effect of EM soil characteristics on TDR waveform

This section discusses an integrated numerical and experimental evaluation of the basic electrical properties of soils on the EM response of TDR systems. First, the materials used in the experimental work are briefly described.

Materials

Table 5 shows the geotechnical characteristics of the materials used in this research. TDR waveforms from previous research at Purdue University conducted by Lin (1999)[13] and Daita (2005)[16] were re-analyzed. As part of this research, 50 additional TDR tests at 20°C with ASTM reference soils were conducted. Daita (2005)[16] used the Campbell Scientific TDR100 that was also used in this research. Lin (1999) [13] used a Tektronix 1502B cable tester.

All of the previous soils were prepared with tap water. After preparing the soil at a desired water content, the materials were sealed with plastic wraps and allowed to equilibrate for more that 24 hours in a humid room to achieve a uniform soil. In order to avoid the effect of temperature on the EM properties of the material being tested (Yu and Drnevich, 2004[2]), before conducting each TDR test, the packaged soil (before compaction) was exposed to a 20°C environment for up to 20 hours to reach temperature equilibrium. After the compaction of the soil, a central rod was driven into the compaction mold. Thus, the compaction mold and the central rod act as the outer and inner conductor, respectively, while the soil act as the insulating material.

Evaluation of electrical soil characteristics

The EM response of the TDR TL is defined by the EM behavior of the soil and the TL characteristics. The permittivity, relaxation frequency, and bulk electric conductivity are related to the soil type, dry density, water content, and pore fluid characteristics. The effects of the

Table 5. Engineering characteristics of the soils used in this research.

Soil	Classification	Sand (%)	Silt (%)	Clay (%)	G_s	P<#200 (%)	LL (%)	PI	TDR waveform source
M1 ‡	SM-SC	55	35	10	2.76	41.3	-	-	Lin (1999)[13]
M2 ‡	ML	37.5	40	17.5	2.77	52.4	16.2	10.5	Lin (1999)[13]
M3 ‡	CL	20	55	25	2.83	72.9	28.5	12.3	Lin (1999)[13]
M4 ‡	CL	12.5	47.5	40	2.83	78.6	33.7	18.9	Lin (1999)[13]
M5 ‡	CL	5	40	55	2.82	84.4	41	19.9	Lin (1999)[13]
Jasper	CL	11	60	29	*	*	47	26	Daita (2005)[16]
Jascrete	CL	50	35	15	*	50.5	24	9	Daita (2005)[16]
Orchard	CL	28	47	25	*	72.2	35	19	Daita (2005)[16]
Salisbury	CL	10	48	42	*	91	48	29	Daita (2005)[16]
Grundite	CL	23	51	25	2.73	76	46.7	26	Daita (2005)[16]
Florida sand	SP	*	*	0	2.65	*	-	-	Drnevich et al. (2005)[17]
Ottawa sand	SP	≈ 100	0	0	2.65	0	-	-	This research
ASTM CH †	CH	16.8	35.8	47.3	2.72	98.8	60	40	This research
ASTM CL †	CL	42.3	27.7	30	2.67	88.5	33.2	13.4	This research
ASTM ML†	ML	1	94	5	2.72	99	29	8	This research

Notation: G_s is the specific gravity. P<#200 is the percentage of soil that pass No.200 sieve. LL is the liquid limit. PI is the plastic index.

Note: *Unknown values. ‡ The percentage of sand, silt and clay reported for M soils represented the percentage by weight of Ottawa sand, natural silt and Illite in a mixture. † ASTM reference soils are being provided by Durham Geo Slope Indicator in cooperation with the ASTM Materials reference Laboratory. www.durhamgeo.com/pdf/m_test-pdf/soil/ref_soil.pdf.

variations of these electrical soil parameters on the TL response is evaluated by modeling waveforms utilizing the forward algorithm summarized in Figure 7, and the TL system parameters estimated from the calibration inversion problem of TDR waveforms (Figure 5 and Tables 3 and 4). The complex EM interaction of the water and soil particles makes it difficult to define a dielectric model capable of modeling the multiple polarization mechanisms that occur especially at frequencies below 1000 MHz (Figure 2). Considering that the purpose of the evaluations here is to study the overall effect of the soil EM properties on the TL response, it is not intended to model the true electrical behavior of the soil. Thus, the Debye dielectric model (Santamarina, J.C. 2001[8]) is adequate. The dielectric permittivity at low (ε_o) and high frequencies (ε_∞), and the relaxation frequency (f_{rel}) define the simplified dielectric spectrum of a dispersive material presented in Figure 8 associated with the Deybe model. Non-dispersive materials are characterized by a flat dielectric spectrum where ε_o and ε_∞ are equal. The numerical analysis is then complemented by the evaluation of TDR laboratory tests with the soils listed in Table 5.

a) Permittivity

The electrical behavior of soils exposed to a time-varying EM field is represented by multiple polarization mechanisms due to the interfacial effects and the EM response of the free water, soil particles and air. The phenomena associated with the interfacial effects include the Maxwell-Wagner polarization and bound water polarization that occur at frequencies below 1 GHz. Being a polar material, the EM responses of free water result in electronic, ionic and orientational polarization in the visible, infrared and microwave frequency range, respectively; non-polar components including soil particles and air only experience electronic and ionic polarization.

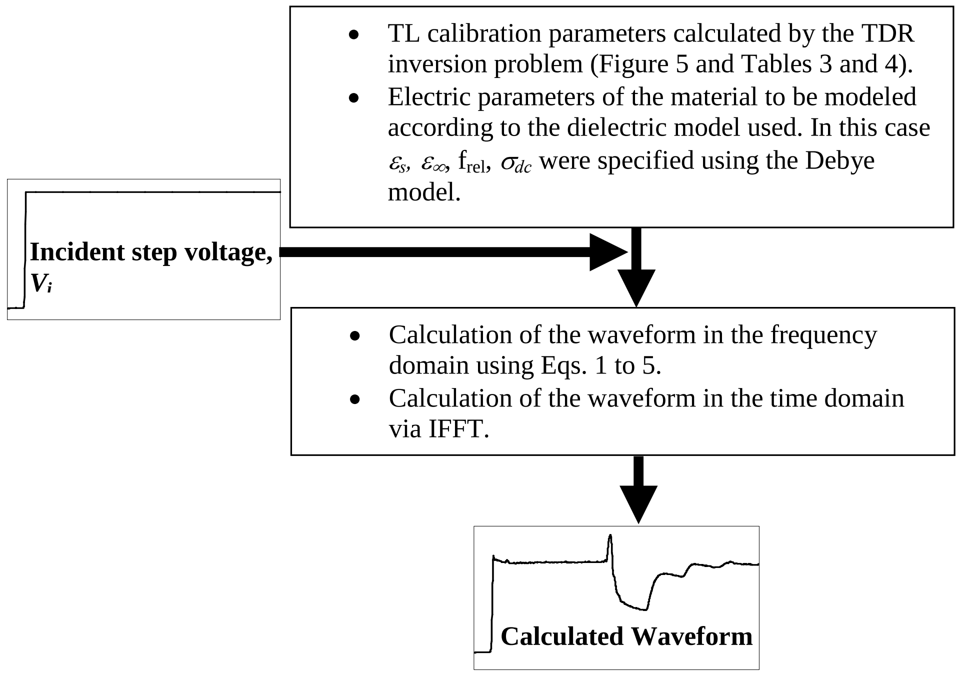

Fig. 7. Simplified flowchart of the forward waveform modeling algorithm

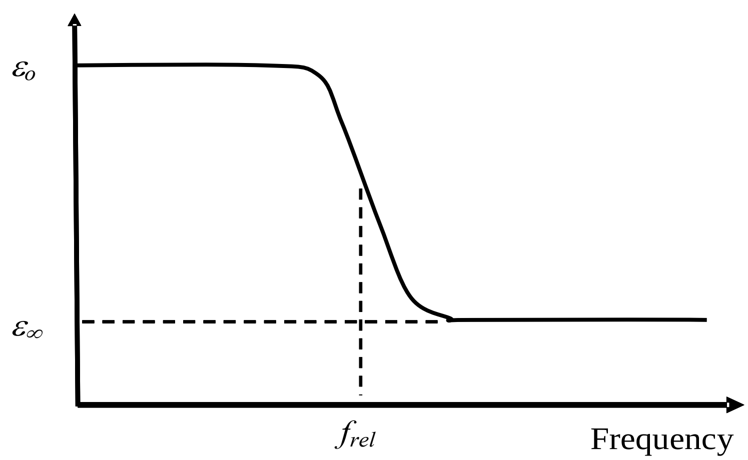

Fig. 8. Real part of the dielectric permittivity using the Debye model

The permittivity of bulk soil mixture increases with the decreasing frequency as the result of the accumulated contribution of these polarization mechanisms (Santamarina, 2001[8]). The apparent dielectric constant (K_a) estimated by travel-time analysis of a typical TDR signal reflects the contribution of the polarization mechanisms associated with frequencies greater than about 1 GHz. Fresh and sea water have a K_a of approximately 80. Air has a K_a of 1. Dry soil solids present a relatively narrow range of K_a between 2 and 7, where the value is controlled by the atomic structure of the crystals and the density of the soil mass. Among different types of soils, the values of K_a normalized by the density is higher for clay minerals than other minerals due to their highly active electrical structure.

The variation of soil permittivity with frequency defines both speed and attenuation of the EM wave in soils. The TDR signal is composed of broadband frequency components. The different frequency components of EM wave travel at the same speed (in phase) in certain materials (referred as non-dispersive); when the EM wave is transmitted into a dispersive material such as soils, the high frequency components of the wave travel faster and attenuate more rapidly. Thus the reflection of high frequent components dominate the TDR signal reflections from the end of the probe section (Robinson et al., 2003[18]). Figure 9 is generated to visualize the effects of the high frequent components. In this figure, two TDR waveforms were simulated in material with a relaxation frequency of 0.8 GHz. Both material 1 and material 2 have an ε_o equal to 25; the ε_∞ values are 4.22 and 20, respectively. The differences in ε_∞ were set deliberately in order to visualize the overall effect of the high frequency components on the TDR signals. From Figure 9 it can be seen that the differences between these waveforms are concentrated in the zones where voltage abruptly increases due to the reflections from the end of the probe section that occurs near 30 ns.

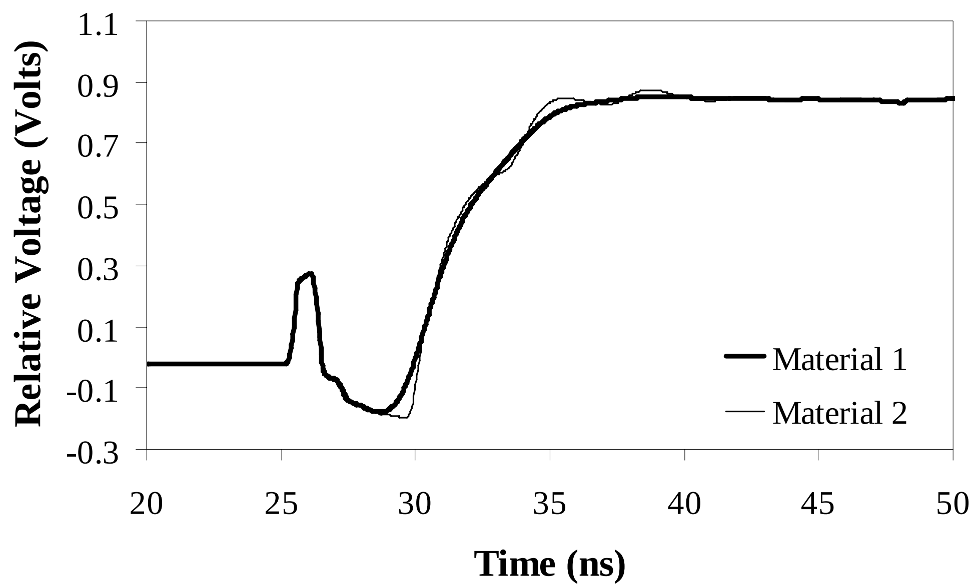

Fig. 9. Modeled TDR waveforms. Material 1 has ε_o and ε_∞ equal to 25 and 4.22, respectively, and Material 2 has ε_o and ε_∞ equal to 25 and 20, respectively. Both materials have a relaxation frequency of 0.8 GHz.

The influence of the static permittivity (ε_o) also was evaluated. Figure 10 shows the modeled TDR waveforms with the electrical parameters of the deionized water (Table 2) where ε_o was systematically varied. A reduction of the negative reflection in the probe can be observed as the static permittivity decreases; this is due to the increase of the characteristic impedance of the probe section (Eq. 7). In sandy materials K_a is close to ε_o as low frequency polarization does not appear due to the poor interfacial interaction between sand grains and water. The modeled waveforms in Figure 10 with K_a equal or less than 50 are representative of sandy materials with different water contents and/or dry densities. From Figure 9 and 10 as well as the discussion above, the TDR waveform for sandy materials is mainly controlled by the low frequent permittivity; the TDR waveform in clayey soils on the other hand is controlled by the polarization process in the high frequency range.

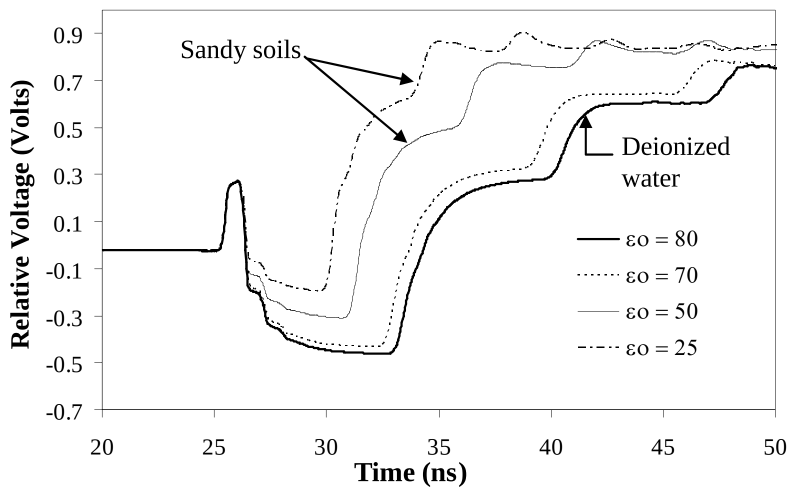

Fig. 10. Effect of the variation of the static permittivity (ε_o) on the sampled TDR signal. The TDR waveform of the deionized water has an ε_o = 80. The numerically modeled waveforms of sandy soils represent soils with different water content and/or dry density. As the water content decreases, ε_o decreases as well.

b) Relaxation Frequency

The relaxation frequency is associated with the soil type. Wet sandy soils present only one relaxation at about 17 GHz, which is related to the free water polarization. Wet clayey and silty soils present additional relaxations below the microwave range due to the interfacial effects (Figure 2). Figure 11 shows two modeled TDR waveforms at low water content with a relaxation frequency outside and inside of the TDR bandwidth (1 GHz). The overall effect of the reduction of the relaxation frequency from 17 GHz to 0.8 GHz is to smooth the waveform and increase the rise time of the first reflection from the probe at approximately 30 ns in Figure 11.

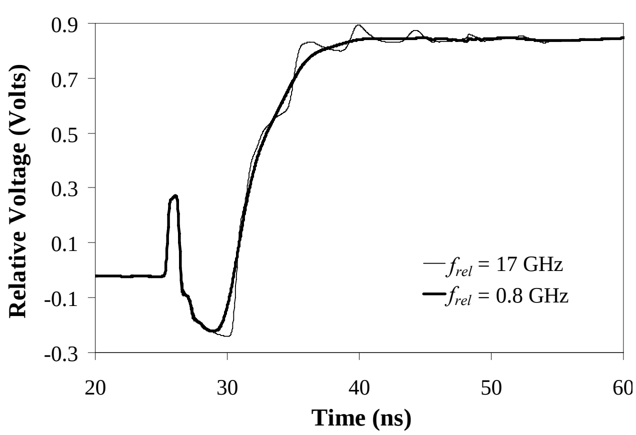

Fig. 11. TDR Waveforms for ε_o = 25, ε_∞ = 4.22, bulk electric conductivity (σ) of zero, and relaxation frequencies (f_{rel}) of 17 GHz and 0.8 GHz associated with the free and bound water polarization, respectively.

Figure 12 shows the observed TDR waveforms of Ottawa sand, ASTM ML, ASTM CL and ASTM CH soils, all oven dried. Due to the absence of water there are not major differences among them. However, the dry density of the specimens differs, being lower in the clay soils, which mask the difference between sand and clay particles as will be discussed later. The steep and high voltage from the end of the probe section in dry specimens is because of the high EM wave velocity that makes the multiple reflections that occur at the coaxial head, soil surface, and the probe section interfere with each other. Figure 13 shows the TDR waveform of the same soils but with water content around 3%. This small amount of water is enough to smooth the waveforms of fine soils due to the reduction of the relaxation frequency associated with the interfacial effects. Figure 14 shows the observed TDR waveforms of these four ASTM soils at high water content, where marked differences in their waveforms is observed due to both the relaxation frequency and the bulk electrical conductivity.

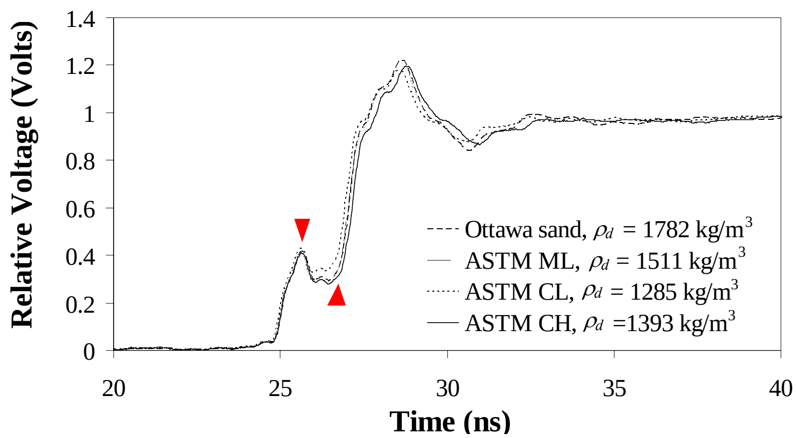

Fig.12. Observed TDR waveforms of oven dry sandy, silty and clayey soils. Mixtures of soil particles and air tend to behave as a non-dispersive material because the values of ε_o and ε_∞ are similar (The initial rise-time of the TDR signal is not shown). The arrows mark the time span of the EM wave first travel through the soil specimen.

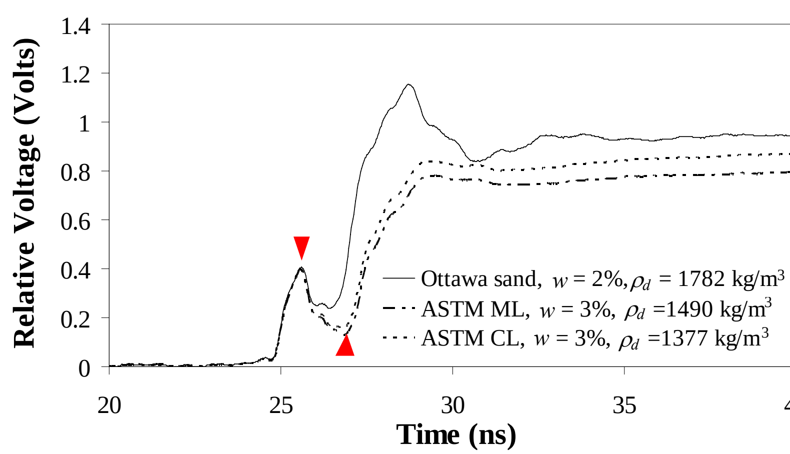

Fig. 13. Observed TDR waveforms of sandy, silty, and clayey soils at low water content (The initial rise-time of the TDR signal is not shown). The arrows mark the time span of the EM wave first travel through the soil specimen.

Time Domain Identification of Soil Texture

A comprehensive characterization of soils by dielectric spectroscopy requires a dielectric model capable of describing the dynamic EM soil-water interaction observed at frequencies below 0.1 GHz. Several dielectric models are available with variable numbers of parameters. However, unsatisfactory results from inverse analysis have been found especially with the models with a large number of parameters, where the non-uniqueness of the solution is most severe (Lin, 2003[6]; Yu et al., 2005[7]). These limitations are not only limited to the performance of the dielectric models but also by the wave propagation mode not being perfectly transverse through

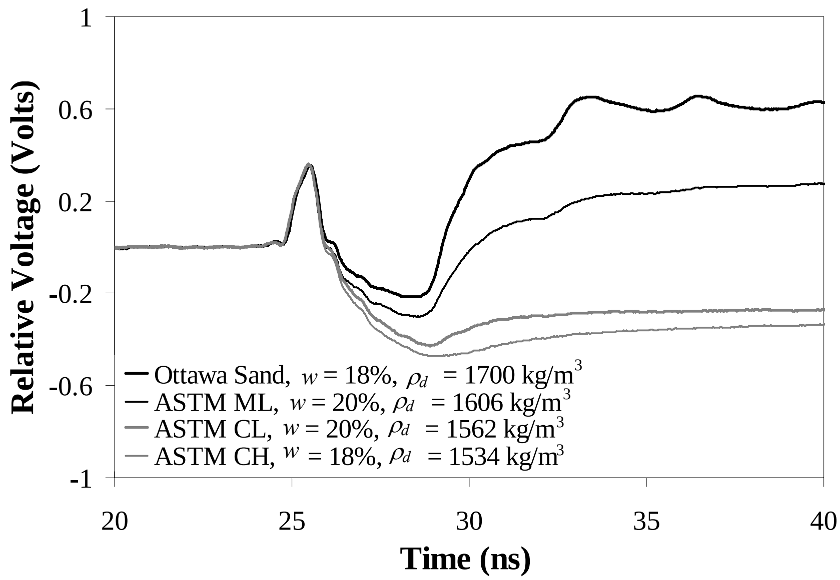

Fig. 14. Observed TDR waveforms of sandy, silty and clayey soils at high water content (The initial rise-time of the TDR signal is not shown).

the TL, due to the high contrast of dielectric properties at the soil surface between the air and the soil being tested (Zambrano et al., 2006[4]). One approach to interpret waveforms is to evaluate TDR waveforms of different soil textures at different water contents, and identify variations in patterns associated with the characteristics of the material being tested, considering that the overall waveform reflects the interplay between porosity, water content, specific surface area, mineralogy, fabric, and pore fluid characteristics. It is desirable to have a simple and efficient empirical approach to identify soil texture that involves interpreting the signal directly in the time domain. Attention will be focused on the first reflection of the wave from the probe section (the portion of the curve immediately to the right of the upward pointing arrows in Figs. 12 through 13) considering that this signal has already been filtered by the soil being tested and is the wave package less attenuated by the electric conductivity and scattering of energy. Figure 15a shows the TDR signal of Ottawa sand with a water content of 6%. Figure 15b is a close up of the first reflection from the end of the probe section and Figure 15c presents the time derivative of this portion of the TDR signal.

The rise time in Figure 15c is related to the relaxation frequency (Figure 11), which is a sensitive parameter for soil texture identification. However, due to the measurement errors and noise induced by taking the time derivative of the TDR signal, the definition of this parameter becomes difficult. Figure 16 shows the relationship between the rise time and the water content for different soil textures. In general the rise time tends to increase with water content.

On the other hand, the area of the pulse delimited by the arrows in Figure 15 is defined by both the K_a and EC_b and by the relaxation frequency of the material (Figures 12 through 14). These electrical parameters are related to the soil texture, water content and pore fluid characteristics. Thus, a simple approach to evaluate the EM behavior of different soils is to study the relationship between the area of the pulse and the water content. Because the end of the pulse is highly affected by a low signal-to-noise ratio, the pulse area is redefined as the zone delimited by the zero crossing point associated with the first reflection from the probe section, and the maximum amplitude of the pulse (Figure15c).

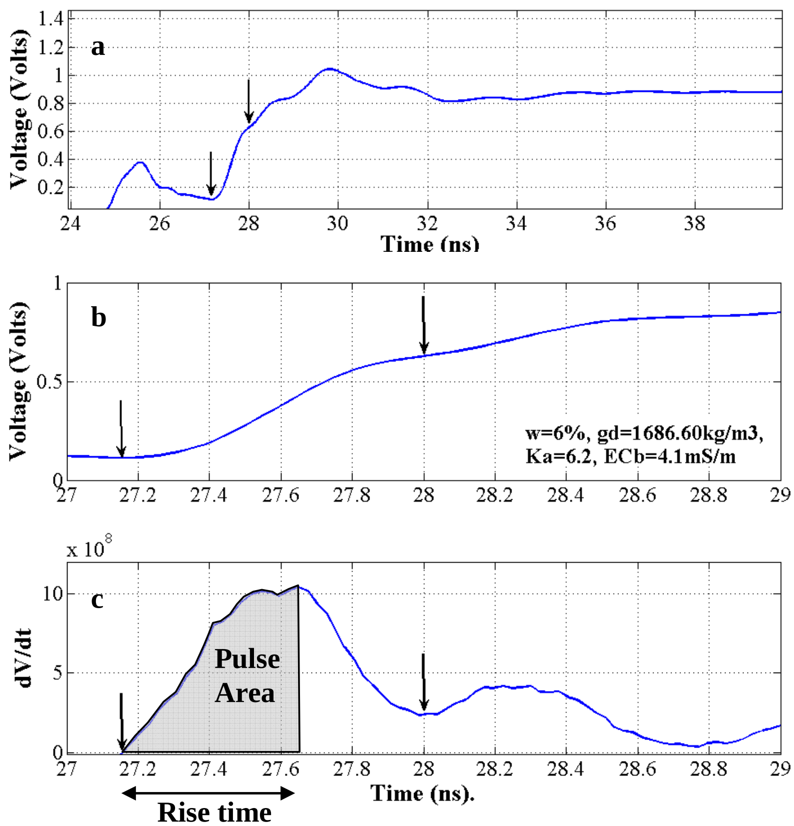

Fig. 15. Determination of the pulse area (PA) and rise time of Ottawa sand with a water content w = 6% and dry density ρ_d = 1686.6 kg/m^3; a) TDR signal. (The arrows mark the reflection to be analyzed); b) Close up of the segment of the wave to be analyzed; and c) Time derivative of the segment of the signal to be analyzed. The shadowed area represents the considered zone of the pulse. The rise time is defined by the starting time of the first reflection and the maximum peak of the pulse.

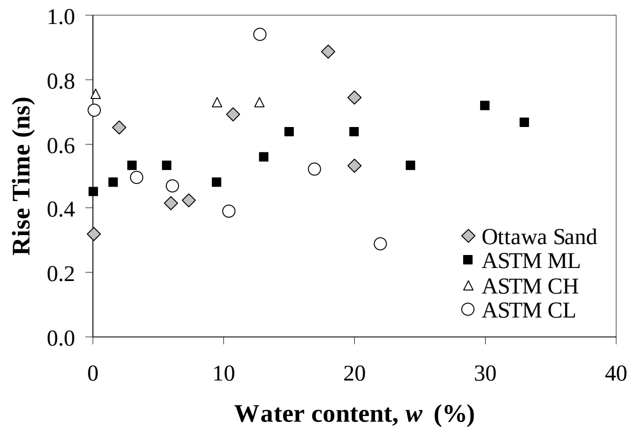

Fig. 16. Variation of rise time with water content for different soil-types at 20°C using tap water.

Figure 17 shows the variation of the pulse area (PA) with water content for different materials. Sandy, silty and clayey soils define three different curves. The uppermost curve is from sands that have a higher pulse area (PA) due to a low EC_b, and high relaxation frequency that allows the K_a to detect more free water. The lowest curve is from clays that have the lowest PA due to the low relaxation frequency and high conductivity. Clayey soils with Liquid Limits less than 50% tend to slightly diverge from the lower curve when the water content exceeds 15%, which shows the effect of the specific surface area (SSA) on the EM response. A transition band between the upper and lower curves is given by silts for water contents greater than 2% as shown by the horizontal arrow in Figure 17. This value is consistent with the minimum amount of water that was found to be required to make difference between coarse and fine soils (compare Figure 13 with Figure 12). In order to evaluate the trends between silts and clays, three mixtures were fabricated with dry Ottawa sand and ASTM CH soil. The 80% Ottawa sand-20% ASTM CH soil mixture is closer to the silt band, while the 50% Ottawa sand-50% ASTM CH soil and the 20% Ottawa sand-80% ASTM CH soil mixtures are near the clay curve.

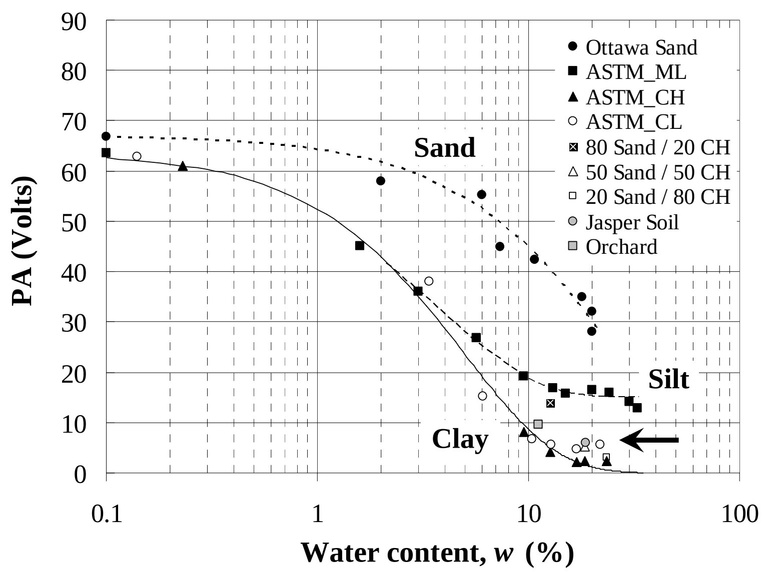

Fig. 17. Variation of the Pulse Area (PA) with water content for different soil types at 20°C using tap water. The arrow indicates the divergence of low and high plastic clays.

Figure 18 shows the relationship between K_a and the dimensionless normalized PA given by the ratio of the PA of the soils to the PA of the input step signal from the cable tester (which is defined as the area from the zero-cross point to the peak of the pulse). This allows the presented relationship to be independent of the voltage magnitude generated by the cable tester. The trends described in Figure 17 for sands, silts and clays are also observed. However, the divergence of clays with a liquid limit higher and lower than 50% is more evident. This chart will allow preliminary soil classification with one TDR test without requiring calibration equations. Increase of the pore fluid conductivity with respect to the tap water will only shift the curves of the clay, silt and sand to the left because the K_a is relatively unaffected by EC_b. However, the effects of porewater conductivity on this approach needs further study.

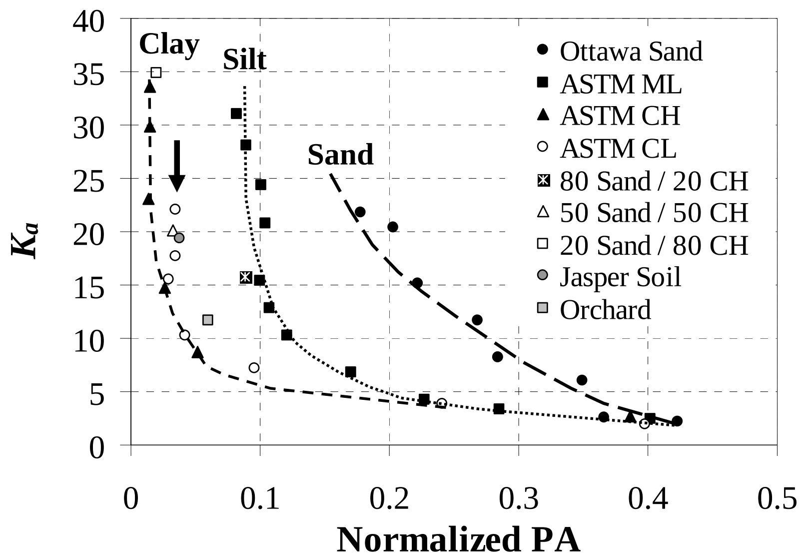

Fig. 18. Variation of K_a with the dimensionless ratio of pulse area (PA) of the soil to the PA of the input step signal. The arrow indicates low plastic clays. This chart will allow conducting preliminary soil classification with one TDR test without requiring calibration equations.

Figure 12 showed that due to the small difference between K_a of air and soil particles, the waveforms of dry clays, dry silts and dry sands do not differ considerably, even if their dry densities are different. A normalization of the pulse area with dry density accounts for the effect of soil particle concentration in a given volume of soil. Figure 19 shows the variation of the density adjusted normalized PA with water content. Following the recommendations of Siddiqui et al. (2000)[1] and Yu and Drnevich (2004)[2] for the dry density compensation of K_a and EC_b, the density adjusted normalized PA is defined by:

$$\text{Density Adjusted Normalized PA} \equiv \sqrt{\frac{PA}{PA_{\text{Input Pulse}}}\frac{\rho_w}{\rho_d}} \qquad (6)$$

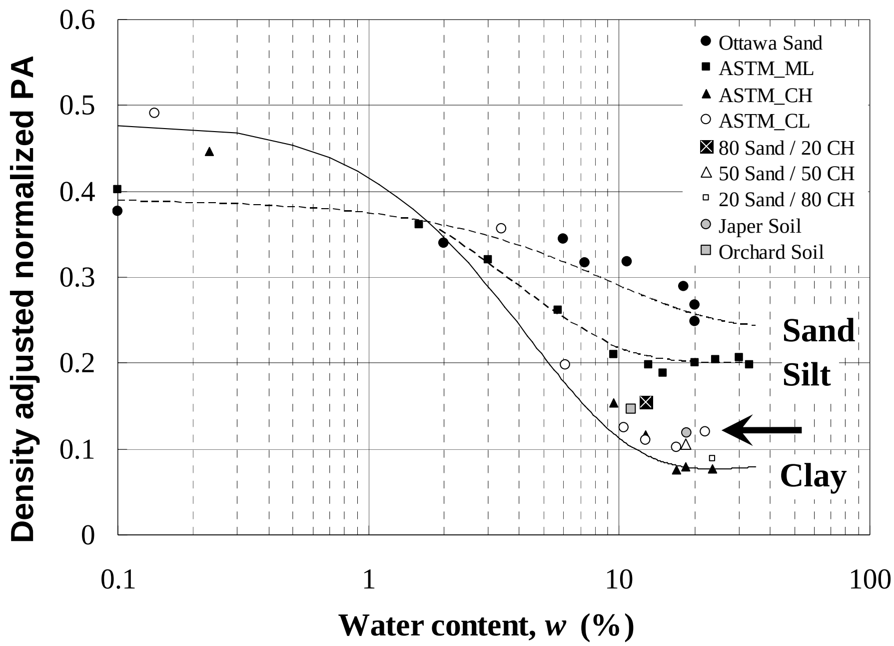

Fig. 19. Variation of the normalized pulse area (PA) adjusted for dry density with water content for different soil types.

Conclusions

TDR estimates water content and dry density based on empirical equations that relate K_a, EC_b, dry density, and water content. Evaluation of TDR tests have revealed that the constants of these equations are soil-type dependent. This paper presents the basis for the extension of the capabilities of the TDR technology for soil texture characterization based on integrated numerical and experimental analysis of sandy, silty and clayey soils. The proposed method overcomes the limitation of dielectric spectroscopy associated with inadequacy of the available dielectric models, and the existence of EM waves that may develop a non-transverse propagation mode at the soil surface.

The proposed model-free method for soil texture characterization analyzes the first reflection from the end of the probe section in the time domain and is based on the detailed description of effects of soil electric properties on the overall configuration of the TDR waveform. The procedure relates the pulse area under the derivative of the reflection from the start of the first reflection to the peak, with the K_a value and water content. The presented time-domain method clearly identifies sands, silts, and clays. At water contents higher than 15% it also appears possible to determine if the clay soil is a low or high plastic clay. The developed methods for soil-type identification from the TDR signal suggest that the TDR system could be self-calibrating. With the use of the developed process, TDR testing could provide material characterization of the tested soil along with water content and density estimation, without requiring sampling or additional laboratory tests. The presented method for soil texture characterization did not consider the effect of changing temperature and/or electrical conductivity of the pore fluid. Research work accounting for these factors in the empirical methods of TDR waveform analysis has already started.

Acknowledgments

The contents of this paper reflect the views of the authors, who are responsible for the facts and the accuracy of the data presented herein, and do not necessarily reflect the official views or policies of the National Science Foundation (Projects: CMS-9907927 and CMS-0244704). The authors are grateful to the National Science Foundation for supporting this research. They also wish to acknowledge Durham Geo – Slope Indicator for providing the ASTM Reference Soils.

References

[1] Siddiqui, S.I., Drnevich, V.P. and Deschamps, R.J. (2000). "Time Domain Reflectometry Development for Use in Geotechnical Engineering." Geotechnical Testing J., 23(1), pp 9-20.

[2] Yu, X. and Drnevich, V.P. (2004). "Soil Water Content and Dry Density by Time Domain Reflectometry." Journal of Geotechnical and Geoenvironmental Engineering, ASCE, Vol. 130, No.9, September, pp 922-934.

[3] Drnevich, V.P, Yu, X., Zambrano, C. and Nowack, R.L. (2006). "Refined One-Step TDR Method for Water Content and Density." GeoCongress 2006, ASCE, Atlanta, 6 p.

[4] Zambrano, C.E. (2006). "Soil Type Identification Using Time Domain Reflectometry.", Thesis in partial fulfillment of the Requirements for the Master of Science in Civil Engineering. Purdue University, 216 p.

[5] ASTM D 6780-05 (2005). "Standard Test Method for Water Content and Density of Soil in Place by Time Domain Reflectometry (TDR)." Annual Book of ASTM Standards, Vol. 04.09.

[6] Lin, C. (2003). "Frequency Domain versus Travel Time Analysis of TDR Waveforms for Soil Moisture Measurements." Soil Science Society of America, J.67, pp 720-729.

[7] Yu, X., Drnevich, V.P., Nowack, R.L. (2005). "Statistical Comparison of Models for Soil Dielectric Spectrum." Geophysical Solutions for Today's Challenges. 18th Annual meeting SAGEEP.

[8] Santamarina, J.C. (2001). "Soils and Waves." John Wiley & Sons, Ltd., 488 p.

[9] Heimovaara, T.J. (1994). "Frequency Domain Analysis of Time Domain Reflectometry Waveforms, 1, Measurement of the complex dielectric permittivity of soils", Water Resources, 30, pp 189-199.

[10] Hilhorst, M.A., Dirksen, F.W., Kampers, F.W., and Feddes, R.A. (2000). "New Dielectric Mixture Equation for Porous Materials Based on Depolarization Factors." Soil Sci. Soc. Am. Journal, 64, pp 1581-1587.

[11] Hilhorst, M.A. and Dirkson, C. (1994). “Dielectric Water Content Sensors: Time Domain versus Frequency Domain.” Symposium and Worshop on Time Domain Reflectometry in Environmental, Infrastructure, and Mining Applications, Evanston, IL, Special Publication, SP 19-94, pp 23-33.

[12] Feng, W., Lin, C.P., Deschamps, R.J. and Drnevich, V.P. (1999a). “Theoretical Model of a Multisection Time Domain Reflectometry Measurement System.” Water Resources Research, 35 (8), pp 2321-2331.

[13] Lin, C-P. (1999). “Time Domain Reflectometry for Soil Properties, Dissertation in partial fulfillment of the Requirements for the Degree Doctor of Philosity.” Pudue Univeristy, p 226.

[14] Huisman, J., Weerts, A., Heimovaara, T., and Bouten, W. (2002). “Comparison of Travel Time Analysis and Inverse Modeling for Soil Water Content Determination with Time Domain Reflectometry.” Water Resource Research. 38, (6), pp 131-138.

[15] Paul, C. (1994). “Analysis of Multiconductors Transmission Lines.” John Wiley & Sons, 559 p.

[16] Daita, R., (2005). “Family of Compaction Curves for Chemically Modified Soils.” Thesis in partial fulfillment of the Requirements for the Master of Science, Purdue Univeristy, May.

[17] Drnevich, V.P., Ashmawy, A.K., Yu, X., and Sallam, A.M. (2005), “Time Domain Reflectometry for Water Content and Density of Soils: Study of Soil-Dependent Calibration Constants”, Canadian Geotechnical Journal, 42, August, pp. 1053-1065.

[18] Robinson, D., Schaap, M., Jones, S., Friedman, S., and Gardner, C. (2003a). “Considerations for Improving the Accuracy of Permittivity Measurement Using Time Domain Reflectometry: Air-Water Calibration, Effects of Cable length.” Soil Science Society of America, J., 67, pp 62-70.

Biographical Information

Carlos E. Zambrano received his B.S. in Civil Engineering from Javeriana University in Bogota, Colombia, his M.S. degree from Purdue University and now works in MWH Global.

Vincent Drnevich obtained his B.S. and M.S. degrees in civil engineering at the University of Notre Dame and his Ph.D. degree from the University of Michigan in Ann Arbor. He was on the civil engineering faculty at the University of Kentucky for 24 years before moving to Purdue University as Professor and Head of Civil Engineering. In 2000, he stepped down from the Head position to devote more time to teaching and research.

Xiong Yu obtained his B.S. and M.S. degree in civil engineering at Tsinghua University and his Ph.D degree from Purdue University. He also holds degrees in computer science and electrical and computer engineering. He is currently a faculty member at department of civil engineering, Case Western Reserve University. His research interests embrace applying interdisciplinary principles to solve a broad spectra of civil engineering problems.

Robert Nowack received a B.A. in Physics at Beloit College, M.S. in Geophysics from Stanford University, and Ph.D. in Geophysics from MIT. He is Professor of Geophysics in the Department of Earth and Atmospheric Sciences at Purdue University.